Electronic Supporting Information for "Spectroscopic characterisation of radical polyinterhalogen molecules"

Joe Gregory,[a] Jan R. R. Verlet[b] and James N. Bull[a]

[a] School of Chemistry, Norwich Research Park, University of East Anglia, Norwich NR4 7TJ, United Kingdom;
E-mail: james.bull@uea.ac.uk
[b] Department of Chemistry, Durham University, South Road, Durham DH1 3LE, United Kingdom

Experimental methods

Experiments were performed using a pulsed valve electric discharge source coupled with a photoelectron imaging spectrometer.[1,2] The seed gas consisted of $\approx$2% CF_3I in argon (Ar) at a total stagnation pressure of $\approx$2.5 Bar. The discharge source, which was based on the design of Neumark and co-workers[3], had a simple three electrode arrangement, combining a Parker series 9 general valve with a discharge chamber of volume $\approx 2\,\mathrm{mm}^3$. The plasma is termed 'hard' due to electric discharge conditions that induce a high degree of ionisation, dissociation and reactions between plasma species. A $\approx$10 mm length, 2 mm diameter bore earthed electrode at the end of the discharge source provided a jet-cooled expansion into vacuum and provided sufficient cooling of plasma species to give small amounts of argon-anion clusters (implies good jet cooling). The jet-cooled expansion was directed between a set of pulsed time-of-flight (ToF) electrodes in an perpendicular arrangement. ToF electrodes were switched to high-voltage using a pair of Behlke switches, accelerating the anions into the time-of-flight region. A series of deflectors and Einzel lenses directed and focussed the ions into a penetrating field velocity-mapping assembly[2] where a pulse of wavelength-tunable light from a YAG-pumped (Continuum Surelite II) optical parametric oscillator (Continuum Horizon I) was timed to interact with a ion packet of a selected mass-to-charge ratio. Velocity-mapping resolution was $\frac{\Delta E}{E} \approx 5\%$, and image reconstructions used anti-aliasing and polar onion peeling algorithms.[4]

Theoretical methods

Electronic structure calculations were performed using the Gaussian 16.B01 software package.[5] Equilibrium geometries were first optimised at the ωB97X-D//def2-TZVPD and MP2//def2-TZVPD levels of theory and confirmed to represent geometrical minima through harmonic vibrational frequency analysis.[6–9] Both ωB97X-D and MP2 methods were used to optimise initial geometries and determine vibrational frequencies to test whether wave function and density function theory methods converged to different minima. The def2-TZVPD and larger def2-QZVPD basis set include an effective core potential function for iodine atoms,[10] approximately treating scalar relativistic effects. This series of basis sets are well parametrised for describing polarisabilities and associated electron densities of each atom, which is an important consideration for the correct description of anions.[8] The minimum energy geometries and vibrational frequencies were reoptimised at the CCSD(T)//def2-TZVPD level of theory.[11] Single-point energies were computed at the CCSD(T)/def2-QZVPD level of theory to assess basis set convergence of the ADE and VDE values. The CCSD(T) level of theory yielded the iodine atomic electron affinity at 3.13 eV (def2-TZVPD basis set) and 3.25 eV (def2-QZVPD basis set), with the former in good agreement with the experimental value of 3.06 eV.[12] The better agreement with experiment for a smaller basis set is presumably from cancellation of errors (Pauling point agreement).

Atomic charges for each anion isomer were computed at the CCSD/def2-TZVPD [CCSD(T)//def2-TZVPD optimised geometries] level of theory using the natural bond order (NBO) scheme as implemented in Gaussian 16.[13]

Vertical excitation energies of anion singlet states were computed at the EOM-CCSD/def2-TZVPD and EOM-CCSD/def2-QZVPD levels of theory assuming optimised geometries for the ground electronic state at the CCSD(T)//def2-TZVPD level of theory.[14]

Simulation of the direct photodetachment spectra for IF_2^- was performed using the Franck-Condon algorithm implemented in Gaussian 16 at the CCSD(T)//def2-TZVPD and (time-dependent) ωB97X-D//def2-TZVPD levels of theory.[15,16]

Species	VEE / eV (f in parentheses)
IF_2^-: [F-I-F]$^-$	B_{2g} & B_{3g}: 4.50 (0.0), B_{1g} & A_g: 5.78 (0.0)
def2-QZVPD	B_{2g} & B_{3g}: 4.51 (0.0), B_{1g} & A_g: 5.69 (0.0)
I_2F^-: [I-I-F]$^-$	B_1 & B_2: 3.59 (7×10^{-3}), B_1 & B_2: 4.80 (3×10^{-3}), A_1: 5.16 (0.9), B_2: 5.46 (0.04)
def2-QZVPD	B_1 & B_2: 3.60 (7×10^{-3}), B_1 & B_2: 4.82 (3×10^{-3}), A_1: 5.21 (0.9), B_2: 5.33 (0.03)
I_2F^-: [I-F-I]$^-$	B_1 & B_2: 2.27 (0.0), B_1 & B_2: 2.53 (3×10^{-4}), A_1: 3.57 (1.5), B_2: 4.88 (0.03)
def2-QZVPD	B_1 & B_2: 2.27 (0.0), B_1 & B_2: 2.54 (2×10^{-4}), A_1: 3.58 (1.5), B_2: 4.81 (1×10^{-3})

Table S1 Calculated vertical excitation energies (VEEs) for IF_2^- and I_2F^- at the EOM-CCSD/def2-TZVPD and EOM-CCSD/def2-QZVPD levels of theory assuming CCSD(T)//def2-TZVPD optimised geometries.

Vertical excitation energies

Vertical excitation energies (VEEs) calculated at the EOM-CCSD/def2-TZVPD and EOM-CCSD/def2-QZVPD [CCSD(T)//def2-TZVPD optimised geometries] levels of theory are given in Table S1. In all cases, the triple-ζ basis set values are close to the quadruple-ζ values, indicating that the vertical excitation energies are roughly converged with basis set size.

Franck-Condon simulations at higher temperature

This section provides further evidence for the ADE assignments in the photoelectron spectra for IF_2^- as the [I-F-I]$^-$ isomer. Briefly, ions produced in the plasma discharge source underwent jet cooling, however, some fraction of vibrationally excited anions may give rise to hot bands. To assess potential contributions from hot bands, we performed Franck-Condon direct photodetachment simulations to form the ground electronic state of the [F-I-F] species (Fig. S1) and to form the A_1 state of the [I-I-F] species (Fig. S1) assuming the temperatures of 100, 200 and 300 K. For [F-I-F], the simulations show that an increase in temperature leads to an increase in hot band intensity and a decrease in intensity of the main Franck-Condon modes. Simulations at higher temperatures (400 and 500 K) show further hot band signal intensity increase and loss of vibrational resolution. For the A_1 state of [I-I-F], the simulations indicate that the vibration denoted by * in Fig. 3a in the paper is due to hot band signal.

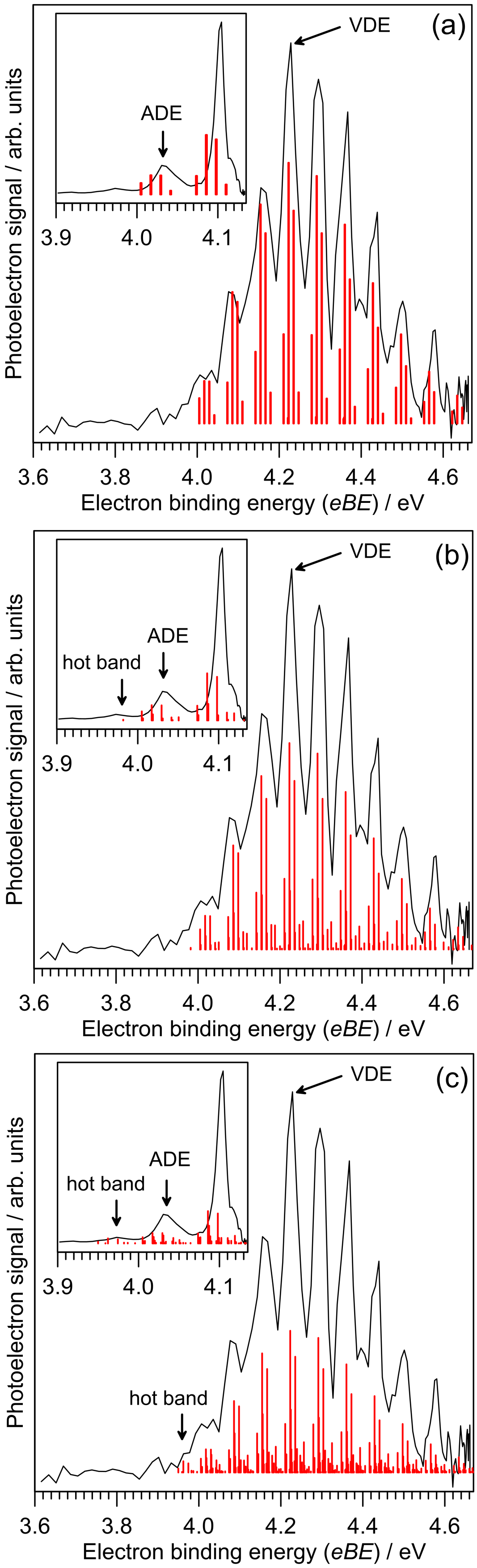

Figure S1 Photoelectron spectra for IF_2^- and Franck-Condon simulations at temperatures of: (a) 100 K, (b) 200 K and (c) 300 K. Weak signal at ≈3.95 eV is consistent with hot bands.

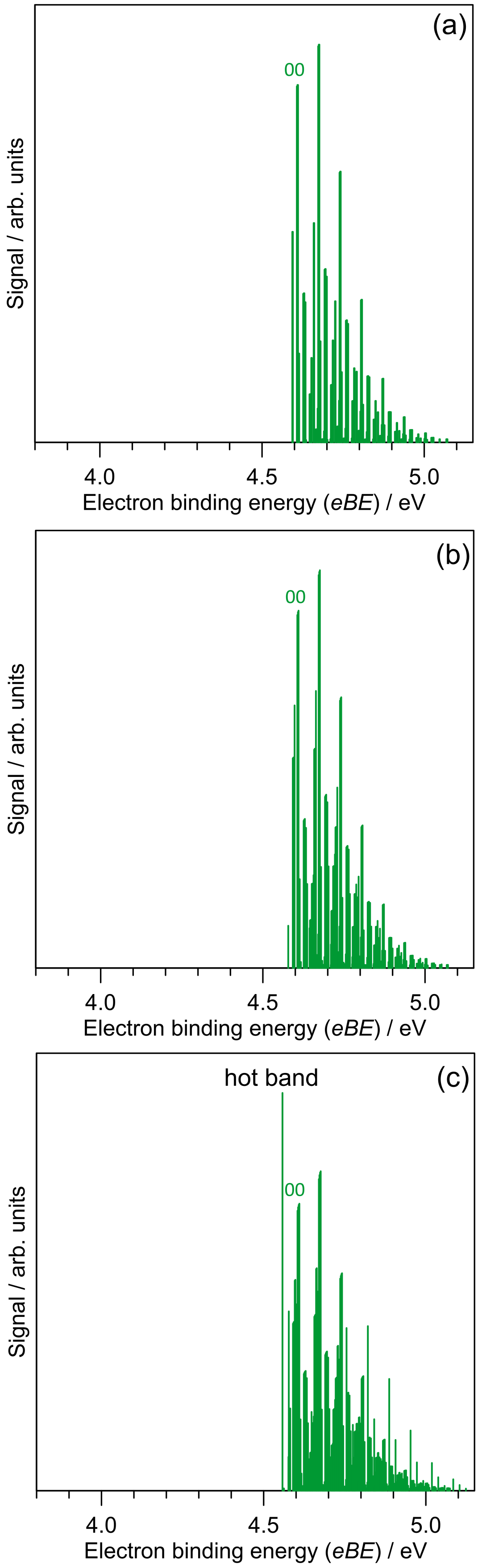

Figure S2 Franck-Condon simulations for photodetachment to form the A_1 state of [I-I-F] at temperatures of: (a) 100 K, (b) 200 K and (c) 300 K. Hot band signal is evident in the 200 and 300 K simulations.

Notes and references

[1] G. M. Roberts, J. Lecointre, D. A. Horke and J. R. R. Verlet, *Phys. Chem. Chem. Phys.*, 2010, **12**, 6226–6232.

[2] D. A. Horke, G. M. Roberts, J. Lecointre and J. R. R. Verlet, *Rev. Sci. Instrum.*, 2012, **83**, 063101.

[3] E. Garand, T. I. Yacovitch and D. M. Neumark, *J. Chem. Phys.*, 2009, **130**, 064304.

[4] G. M. Roberts, J. L. Nixon, J. Lecointre, E. Wrede and J. R. R. Verlet, *Rev. Sci. Instrum.*, 2009, **80**, 053104.

[5] M. J. Frisch, G. W. Trucks, H. B. Schlegel, G. E. Scuseria, M. A. Robb, J. R. Cheeseman, G. Scalmani, V. Barone, B. Mennucci, G. A. Petersson, H. Nakatsuji, M. Caricato, X. Li, H. P. Hratchian, A. F. Izmaylov, J. Bloino, G. Zheng, J. L. Sonnenberg, M. Hada, M. Ehara, K. Toyota, R. Fukuda, J. Hasegawa, M. Ishida, T. Nakajima, Y. Honda, O. Kitao, H. Nakai, T. Vreven, J. A. Montgomery, Jr., J. E. Peralta, F. Ogliaro, M. Bearpark, J. J. Heyd, E. Brothers, K. N. Kudin, V. N. Staroverov, R. Kobayashi, J. Normand, K. Raghavachari, A. Rendell, J. C. Burant, S. S. Iyengar, J. Tomasi, M. Cossi, N. Rega, J. M. Millam, M. Klene, J. E. Knox, J. B. Cross, V. Bakken, C. Adamo, J. Jaramillo, R. Gomperts, R. E. Stratmann, O. Yazyev, A. J. Austin, R. Cammi, C. Pomelli, J. W. Ochterski, R. L. Martin, K. Morokuma, V. G. Zakrzewski, G. A. Voth, P. Salvador, J. J. Dannenberg, S. Dapprich, A. D. Daniels, Ö. Farkas, J. B. Foresman, J. V. Ortiz, J. Cioslowski and D. J. Fox, *Gaussian 16 Revision B.01*, Gaussian Inc. Wallingford CT 2016.

[6] J.-D. Chai and M. Head-Gordon, *Phys. Chem. Chem. Phys.*, 2008, **10**, 6615–6620.

[7] F. Weigend and R. Ahlrichs, *Phys. Chem. Chem. Phys.*, 2005, **7**, 3297.

[8] D. Rappoport and F. Furche, *J. Chem. Phys.*, 2010, **133**, 134105.

[9] M. Head-Gordon and T. Head-Gordon, *Chem. Phys. Lett.*, 1994, **220**, 122–128.

[10] K. A. Peterson, D. Figgen, E. Goll, H. Stoll and M. Dolg, *J. Chem. Phys.*, 2003, **119**, 11113–11123.

[11] J. A. Pople, M. Head-Gordon and K. Raghavachari, *J. Chem. Phys.*, 1987, **87**, 5968–5975.

[12] R. J. Peláez, C. Blondel, C. Delsart and C. Drag, *J. Phys. B: At. Mol. Opt. Phys.*, 2009, **42**, 125001.

[13] A. E. Reed, L. A. Curtiss and F. Weinhold, *Chem. Rev.*, 1988, **88**, 899–926.

[14] J. F. Stanton and R. Bartlett, *J. Chem. Phys.*, 1993, **98**, 7029.

[15] F. Santoro, A. Lami, R. Improta, J. Bloino and V. Barone, *J. Chem. Phys.*, 2008, **128**, 224311.

[16] V. Barone, J. Bloino, M. Biczysko and F. Santoro, *J. Chem. Theo. Comp.*, 2009, **5**, 540–554.